Stratospheric transport by planetary wave mixing as observed during CRISTA-2

M. Riese,[1,4] G. L. Manney,[2] J. Oberheide,[1,5] X. Tie,[3] R. Spang,[1,6] and V. Küll[1]

[1] Planetary waves drive the mean meridional circulation of the stratosphere and at the same time facilitate quasi-horizontal mixing of trace gases. This paper presents significant day-to-day variability of stratospheric trace gas fields associated with large planetary wave activity observed during the second mission of the Cryogenic Infrared Spectrometers and Telescopes for the Atmosphere (CRISTA) experiment. Geopotential height data of the UK Met Office show that the CRISTA-2 observations in the Southern Hemisphere winter were made during a period of extremely large amplitudes of both wave-1 and wave-2. The planetary wave-1, usually a quasi-stationary feature, moved eastward with the traveling planetary wave-2. The large amplitudes of both wave-1 and wave-2 led to a significant displacement of the edge of the polar vortex toward the tropics (down to 30°S). As a result of the large wave amplitudes and favorable phase alignment, the anticyclone drawing up tropical air was unusually strong, and thus considerable wave-induced trace gas flux from the tropics toward midlatitudes was observed, mainly in the form of a pronounced planetary-scale tongue advected out of the tropics around the vortex and into the anticyclone. Quantitative transport calculations based on a sequential data assimilation system highlight the importance of such transport events for trace gas eddy-flux in the Southern Hemisphere winter stratosphere.   INDEX TERMS: 0341 Atmospheric Composition and Structure: Middle atmosphere—constituent transport and chemistry (3334); 3360 Meteorology and Atmospheric Dynamics: Remote sensing; 3364 Meteorology and Atmospheric Dynamics: Synoptic-scale meteorology

1. Introduction

[2] Planetary waves are of great importance for the large-scale dynamics of the middle atmosphere. In the winter hemisphere, mass is transported poleward as a result of planetary wave breaking in the stratospheric surf-zone [e.g., *McIntyre and Palmer*, 1983]. Conservation of mass leads to downward motion in the polar region and upward motion in the tropics, whereby the mean vertical velocity at a given level is mainly controlled by the integrated wave dissipation above this level (downward control principle) [e.g., *Haynes et al.*, 1991]. The horizontal mass exchange between the tropics and midlatitudes is restricted due to a transport barrier located in the subtropics [e.g., *Trepte et al.*, 1993]. Global satellite observations indicate that significant parts of the remaining transport occurs in form of tongues of

tropical air [e.g., *Randel et al.*, 1993]. *Waugh* [1993, 1996] showed that tongues of tropical air drawn into midlatitudes were linked to disturbances of the polar vortex caused by planetary wave activity. Such structures play an important role in slow seasonal and fast day-to-day variations of stratospheric trace gas fields [e.g., *Randel et al.*, 1994]. This paper focuses on rapid daily variability of stratospheric trace gas fields associated with strong planetary wave activity encountered by the Cryogenic Infrared Spectrometers and Telescopes for the Atmosphere 2 (CRISTA-2) experiment in the first half of August 1997 [*Grossmann et al.*, 2002]. The CRISTA trace gas fields are of high spatial resolution in three dimensions, and therefore especially suited to detailed studies of dynamical structures in trace gas fields.

[3] In winter, meridional tracer gradients around the subtropical transport barrier become tightened and the barrier is shifted toward lower latitudes [e.g., *Randel et al.*, 1994]. The CRISTA-2 mission was performed after this transition phase, in a period usually characterized by relatively undisturbed trace gas background fields. However, equatorward displacement of the south polar vortex to latitudes of about 30°S, associated with enhanced planetary wave activity, resulted in relatively high day-to-day variability of stratospheric tracer fields. Significant wave-induced trace gas fluxes occurred in the altitude region of largest wave amplitudes, mainly in the form of a pronounced planetary-scale tongue advected out of

---
[1]Physics Department, University of Wuppertal, Wuppertal, Germany.
[2]Jet Propulsion Laboratory, California Institute of Technology, Pasadena, California, USA.
[3]National Center for Atmospheric Research, Boulder, Colorado, USA.
[4]Now at Research Centre Jülich, ICG-I: Stratosphere, Germany.
[5]Now at National Center for Atmospheric Research, Boulder, Colorado, USA.
[6]Now at EOS Space Research Centre, Leicester, UK.
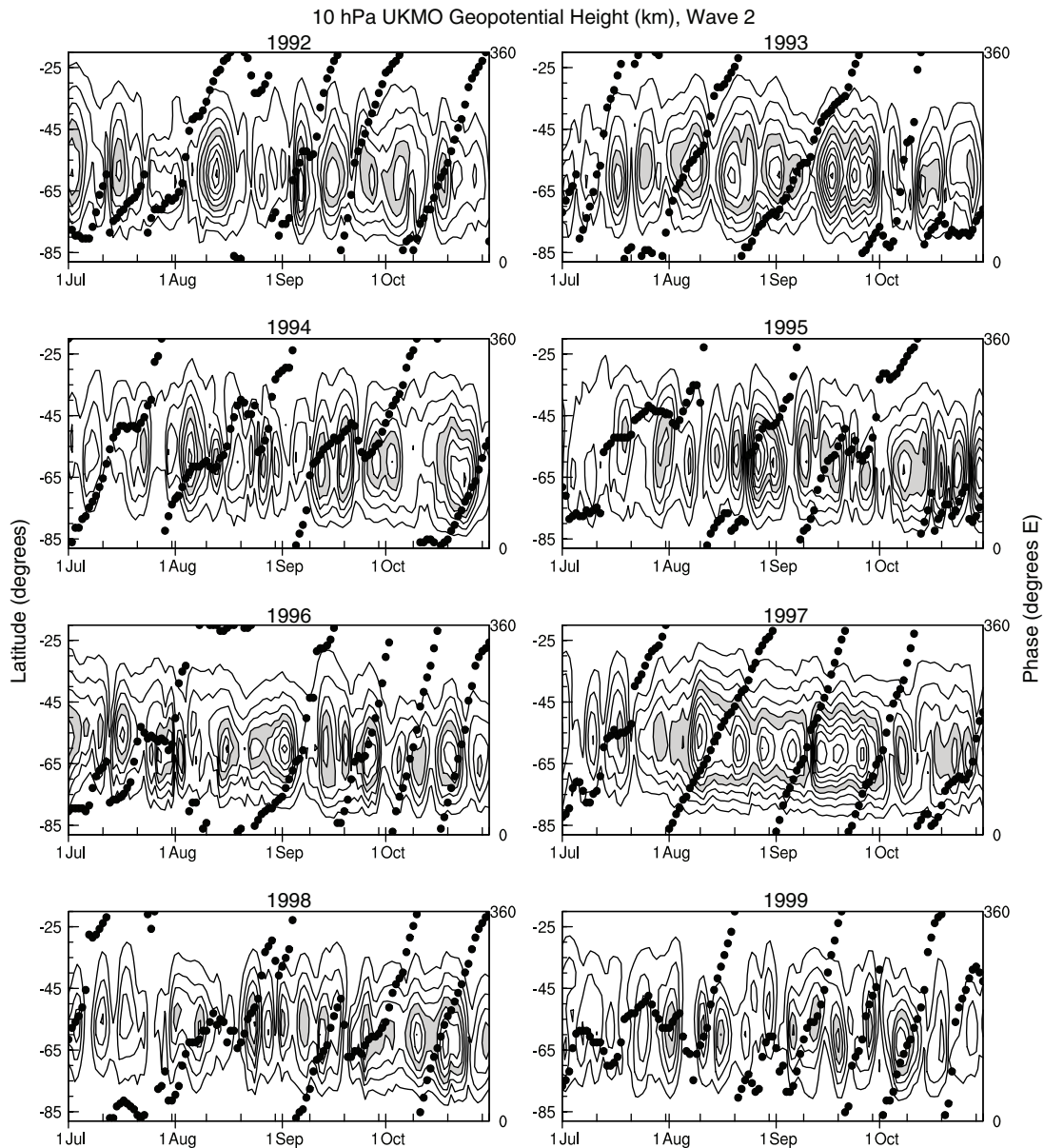
10 hPa UKMO Geopotential Height (km), Wave 2

Figure 1. Time-latitude contour plots of wave-2 geopotential height amplitude at 10 hPa for 1 July through 31 October, 1992 through 1999. The contour interval is 100 m, with 400 to 500 m shaded. The black dots show the phase at 60°S. Phases are plotted at the longitude of one of the two maxima. Note the constancy of the eastward propagation of wave-2 over a long period in 1997. This constancy further emphasizes the unusual wave-2 amplification during the measurement period of CRISTA-2 (9 through 16 August 1997).

the tropics toward midlatitudes. CRISTA-2 observations provide a detailed view of the wave-induced trace gas flux and, in particular, the role of the magnitude of the wave amplitudes and the wave phases.

[4] Section 2 gives a brief description of the CRISTA instrument and its second mission in August 1997. The unusually large planetary wave activity during the CRISTA-2 observational period is demonstrated in section 3.1 by means of time series of wave-1 and wave-2 amplitudes obtained from a spectral analysis of geopotential height fields provided by the UK Met Office (UKMO) [see *Swinbank and O'Neill*, 1994]. Amplitudes of planetary wave-1 and wave-2 for the Southern Hemisphere winter of 1997 are compared

with those of other winters during 1992 through 1999. The dynamics of the strong wave event during CRISTA-2 is investigated in section 3.2 by means of the temporal development of the Eliassen-Palm (EP) flux. A qualitative discussion of the associated fluxes of stratospheric trace gases observed by CRISTA-2 and their relationship to the wave-1 and wave-2 amplitudes is given in section 4. Wave-1 and wave-2 amplitudes and phases control the maximum displacement of the South polar vortex toward the tropics, and therefore the strength of tracer fluxes from the tropics to midlatitudes. Section 5 presents quantitative calculations of nitrous oxide (N_2O) eddy fluxes calculated from synoptic trace gas fields obtained from sequential assimilation of the
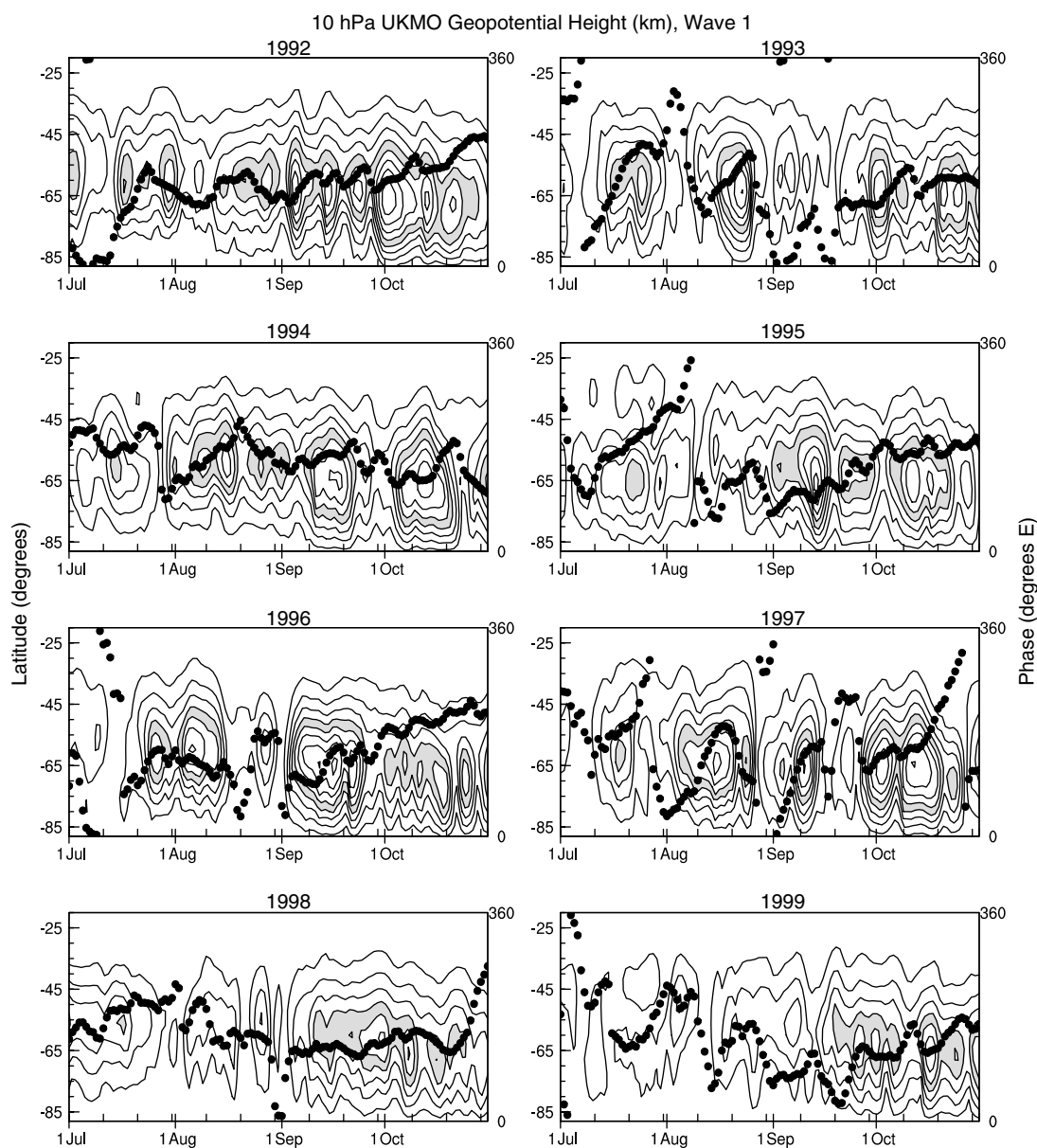
Figure 2. Time-latitude contour plots of wave-1 geopotential height amplitude at 10 hPa for 1 July through 31 October, 1992 through 1999. The contour interval is 200 m, with 800 to 1000 m shaded. The black dots show the phase at 60°S. They are plotted at the longitude of the wave maximum. During CRISTA-2, the position of the wave-1 maximum almost coincides with the position of one of the two wave-2 maxima. This phase alignment produces a strong anticyclone (see also Figure 6), which facilitates significant transport of tropical air toward midlatitudes.

asynoptic CRISTA-2 observations into a chemical transport model (CTM).

2. CRISTA-2 Observations

[5] The CRISTA experiment was flown on the Space Shuttle missions STS 66 in November 1994 and STS 85 in August 1997. The instrument utilizes the limb-scanning technique to measure global distributions of thermal emissions of selected trace gases. CRISTA is mounted on the CRISTA-SPAS satellite which is released from the Shuttle and operates at a distance of 50–100 km behind it.

Measurements are taken during a free-flying period of about a week. For high horizontal resolution CRISTA uses three telescopes that sense the atmosphere simultaneously. This yields high horizontal resolution of typically 3° in latitude and 6° in longitude. The horizontal distance between two measurement points along the flight track is 200 to 400 km, depending on the measurement mode. At the equator, the resolution in the perpendicular horizontal direction is on the order of the separation of the tangent points of the three telescopes (650 km). It becomes much higher at high latitudes. The vertical resolution of the measurements is about 2.5 km. A detailed instrument description is given by

Offermann et al. [1999]. The data processing and the retrieval of atmospheric pressures, temperatures, and trace gas mixing ratio values are described by *Riese et al.* [1999a].

[6] This paper presents version-1 data from the second CRISTA mission. The instrument was operated for eight days (9 August through 16 August) and measured about 45,000 vertical profiles of numerous trace gases from a 300 km, 57° inclination orbit by using a number of different measurement modes [see *Grossmann et al.*, 2002]. The latitudinal coverage of the observations was extended with respect to the orbit inclination by utilizing the maneuvering capabilities of the CRISTA-SPAS satellite. The viewing direction of CRISTA-2 was tilted northward in the northern parts of the orbits and southward in the southern parts of the orbits. This way, a latitudinal coverage from 74°S through 74°N was achieved.

3. Planetary Wave Activity in the Southern Hemisphere Winter Stratosphere

3.1. Wave-1 and Wave-2 Amplitudes at 10 hPa From 1992 to 1999

[7] Planetary waves are always present in the winter stratosphere with highly variable amplitudes and phases. While the wave-1 is usually quasi-stationary in both hemispheres, wave-2 exhibits an interhemispheric asymmetry [e.g., *Leovy and Webster*, 1976; *Manney et al.*, 1991; and references therein]. It is typically quasi-stationary in the Northern Hemisphere and eastward moving in the Southern Hemisphere. *Manney et al.* [1991] investigated the behavior of wave-1 and wave-2 in the Southern Hemisphere for 1 August through 31 October for 10 years, 1979 through 1988, based on daily fields of geopotential height and temperature compiled by the US National Meteorological Center (NMC, now NCEP). The general wave-2 characteristics during this 10-year period can be summarized as follows: wave-2 in the Southern Hemisphere winter mid-stratosphere has a broad meridional structure. Largest wave-2 power is observed around 60°S, with little variation of the latitude of the maximum amplitude throughout the season. Wave-2 propagates eastward with periods ranging from 5 to 40 days. The periods appear to cluster around 20- to 30-day periods and faster 5- to 12-day periods.

[8] These findings are in general agreement with results obtained from a spectral analysis of geopotential height fields for 1992 through 1999 based on meteorological data provided by the UK Met Office. Figures 1 and 2 present time-latitude contour plots of wave-2 and wave-1 geopotential height amplitudes at 10 hPa for each year of the analysis for 1 July through 31 October. The amplitude distributions illustrate the large interannual variability in maximum of amplitudes and timing of largest amplitudes. Time-height contour plots at 60°N of wave amplitudes in 1997 are shown in Figure 3. CRISTA-2 observations (8 August through 16 August) were made during a relatively prolonged period of extremely large wave-2 amplitudes. The situation was further characterized by strong positive correlation with planetary wave-1. Wave-1 amplitudes were rather large during the whole observational period of CRISTA-2. Wave-1 and wave-2 were traveling eastward in phase during CRISTA-2, with the wave-1 max-
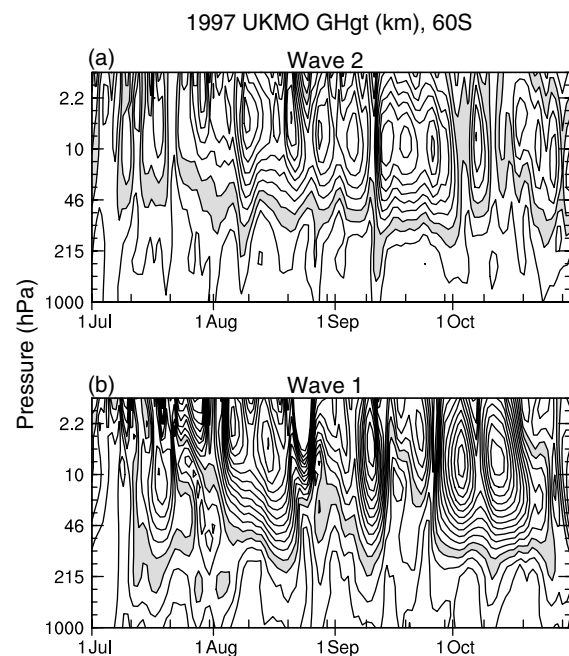

Figure 3. (a) Time-height cross-sections at 60°S of wave-2 geopotential height amplitudes for 1 July through 31 October 1997. Contour interval is 100 m, with 200 to 300 m shaded. (b) Same as in (a) but for wave-1. Contour interval is 100 m, with 300 to 400 m shaded.

imum aligned with one wave-2 maximum (see Figures 1 and 2).

3.2. Wave Dynamics During CRISTA-2

[9] Figures 1, 2, and 3 illustrate wave-1 and wave-2 amplification in late July and early August. While wave-1 already exhibits relatively large amplitude at the beginning of the CRISTA-2 measurement period, wave-2 is still rapidly growing and reaches maximum amplitude around 10 August. The dynamical aspects of the wave growth are shown in Figure 4 in terms of the Eliassen-Palm (EP) flux. On 8 August strong vertical wave propagation (predominantly wave-2) can be seen in the upper troposphere and in the stratosphere. On 10 August enhanced equatorward propagation of wave-2 occurs in the middle stratosphere (around 10 hPa). As time proceeds (12 August, 14 August) EP fluxes in the stratosphere are weakened and the largest fraction of upward propagation shifts from wave-2 to wave-1. This is consistent with wave-2 amplification seen in Figure 1 during the first few days of the CRISTA-2 mission, and wave-1 amplification seen in Figure 2 during the second half of the CRISTA-2 mission. The relationship of these different phases of the wave evolution to trace gas fluxes observed by CRISTA-2 is discussed in section 4.

[10] As mentioned above, wave-1 is usually quasi-stationary. *Manney et al.* [1991] report a limited number of 4 to 10 day periods in the Southern Hemisphere when wave-1 moved eastward with wave-2. However, such events were found in the 1979 through 1988 period only when wave-1 amplitudes were moderate or small (<1000 m). During the CRISTA-2 observational period the planetary wave-1 exhibited large amplitudes but nevertheless traveled east-
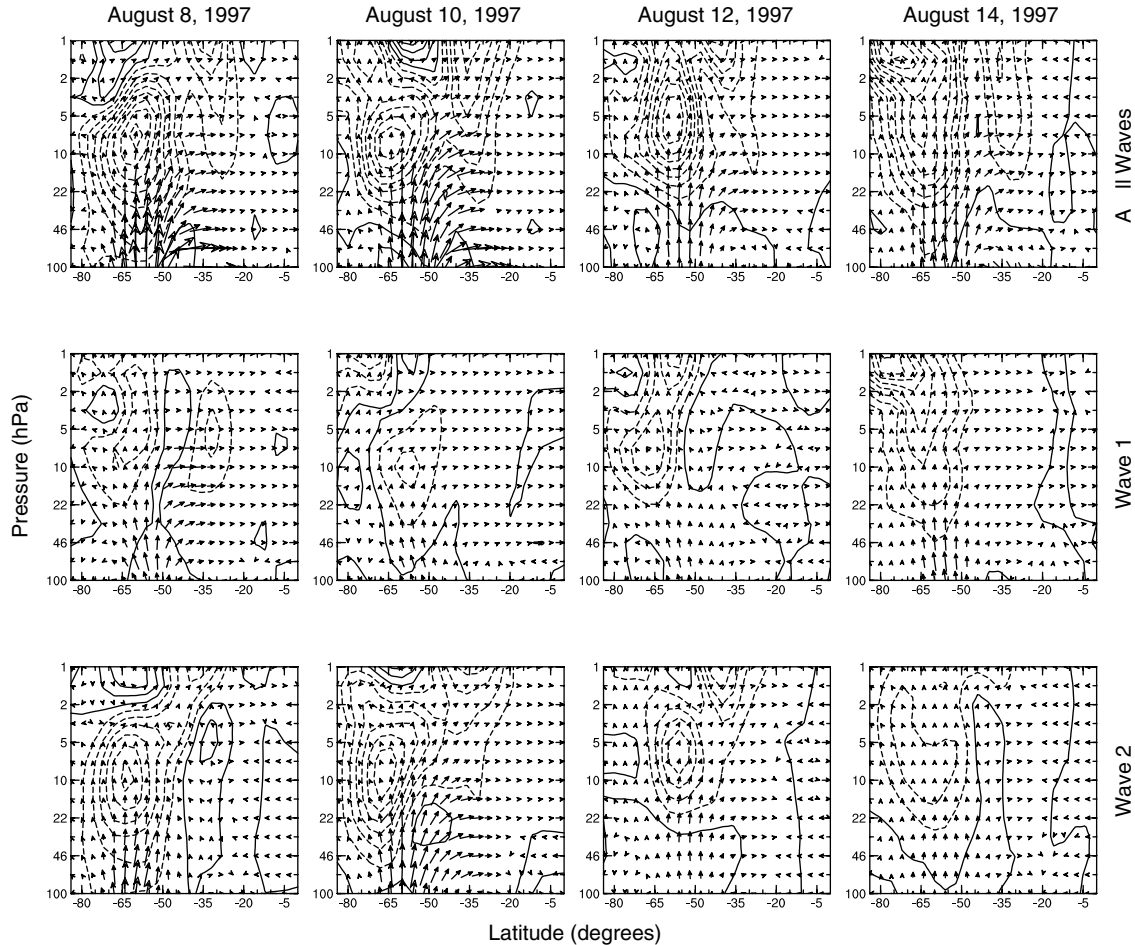
Figure 4. Eliassen-Palm (EP) flux and EP flux divergence for 8, 10, 12, and 14 August 1997. Total fluxes and total divergences (top row) are shown, as well as contributions of wave-1 (middle row) and wave-2 (bottom row). The maximum size EP flux arrow is 7.0×10^{12} kg m s^{-2}. The divergence contour interval is 3 m s^{-1} day^{-1}, with negative values indicated by dashed lines.

ward with wave-2 (Figure 2). This behavior is illustrated in Figure 5 in geopotential height fields derived from CRISTA-2 observations of atmospheric pressure and geometric height distributions [*Oberheide et al.*, 2002]. The planetary wave activity results in a south polar vortex that is shifted off the pole (wave-1) and elongated (wave-2). The extremely large amplitudes of both wave-1 and wave-2 result in a significant displacement of the edge of the polar vortex toward the tropics. The role of this displacement in the formation of planetary-scale tongues of tropical air (transported to midlatitudes) is discussed in section 4.

4. Tracer Transport Observed by CRISTA-2

4.1. Time Sequence of Observed N$_2$O Distributions at 10 hPa

[11] CRISTA-2 observations show that the enhanced equatorward propagation of wave-2 around 10 August (see Figure 4) is accompanied by a strong eddy flux of tracers, mainly in the form of a planetary-scale tongue of tropical air. A time sequence of N$_2$O mixing ratios at 10 hPa observed during CRISTA-2 (10 August through 15 August) is shown in Figure 6. The background distribution of the equatorial N$_2$O mixing ratios is in good agreement with previous observations of the Southern Hemisphere winter stratosphere and results obtained from global circulation models for this particular season [see *Randel et al.*, 1994]. Maximum N$_2$O values are centered somewhat north of the equator (see also Figure 9). Mixing ratio gradients in the area of the subtropical transport barrier are tightened and shifted equatorward. This can be seen, for example, on 10 August in the longitudinal region around 90°E, which is not significantly influenced by the displaced polar vortex.

[12] CRISTA-2 observations, in contrast to climatological results, do not show an approximately symmetric, pole-centered Southern Hemisphere polar vortex with depleted tracer mixing ratios southward of about 60°S. The south polar vortex is shifted off the pole (wave-1) and elongated (wave-2), such that its edge reaches latitudes down to 30°S. The wave structures may be identified in Figure 6 by very low N$_2$O mixing ratios at middle and high southern latitudes. The shape of the low N$_2$O region resembles that of the corresponding geopotential height field shown in Figure 5, and corresponds well with the region of high-magnitude potential vorticity (not shown) that is commonly used to identify the polar vortex.
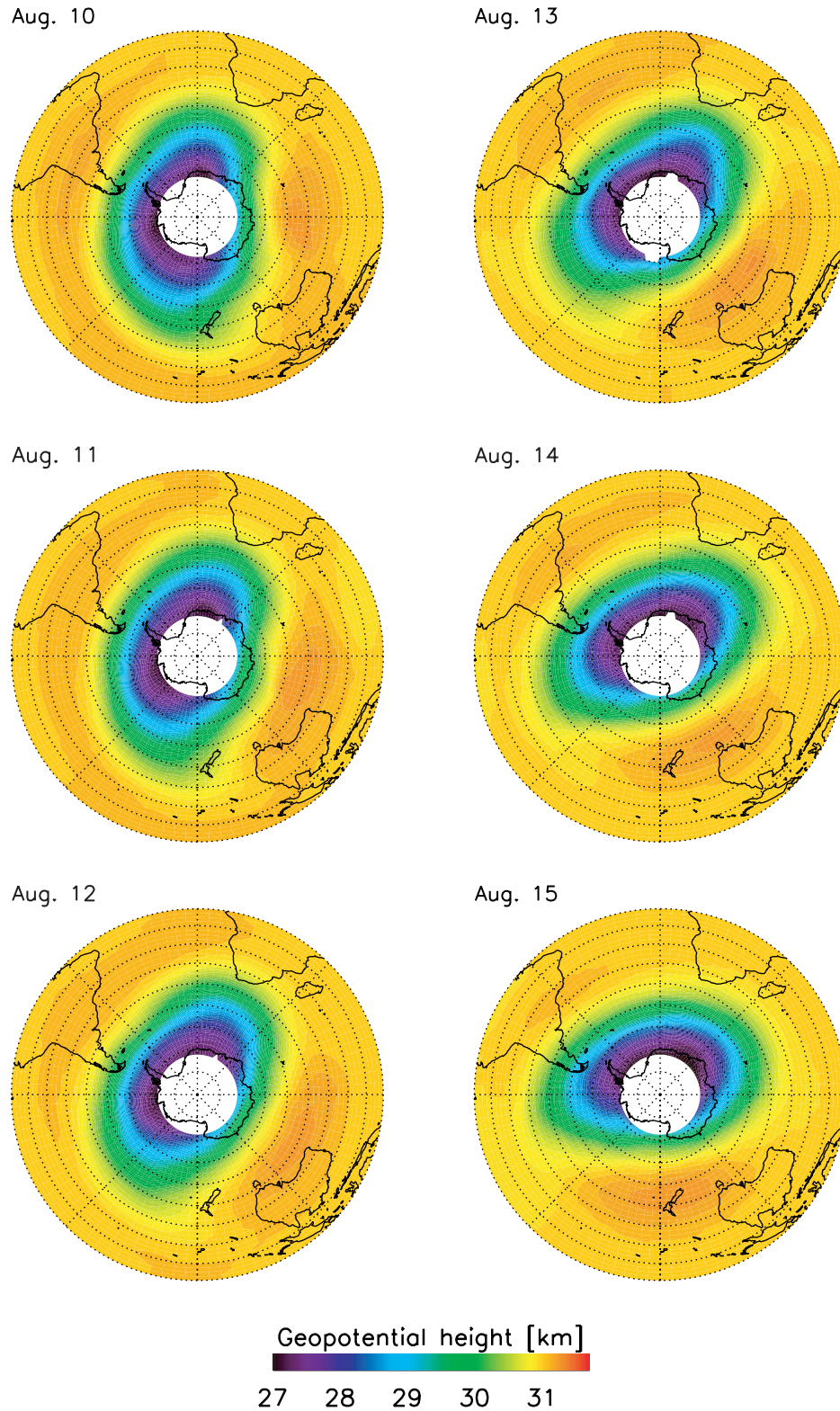
Figure 5. Time sequence (10 August to 15 August 1997) of geopotential height fields at 10 hPa in the Southern Hemisphere derived from CRISTA-2 observations of pressure and geometric height.

[13] The large-scale wind field associated with the wave-disturbed vortex advects air out of the tropics. The details of the disturbed polar vortex are as follows: on 10 August, the wave-2 structure results in a shift of the edge of the vortex toward the tropics at two locations, at the date line and at the Greenwich meridian. The interaction between the vortex and the tropics is most pronounced in the area of the strongest vortex elongation (at the date
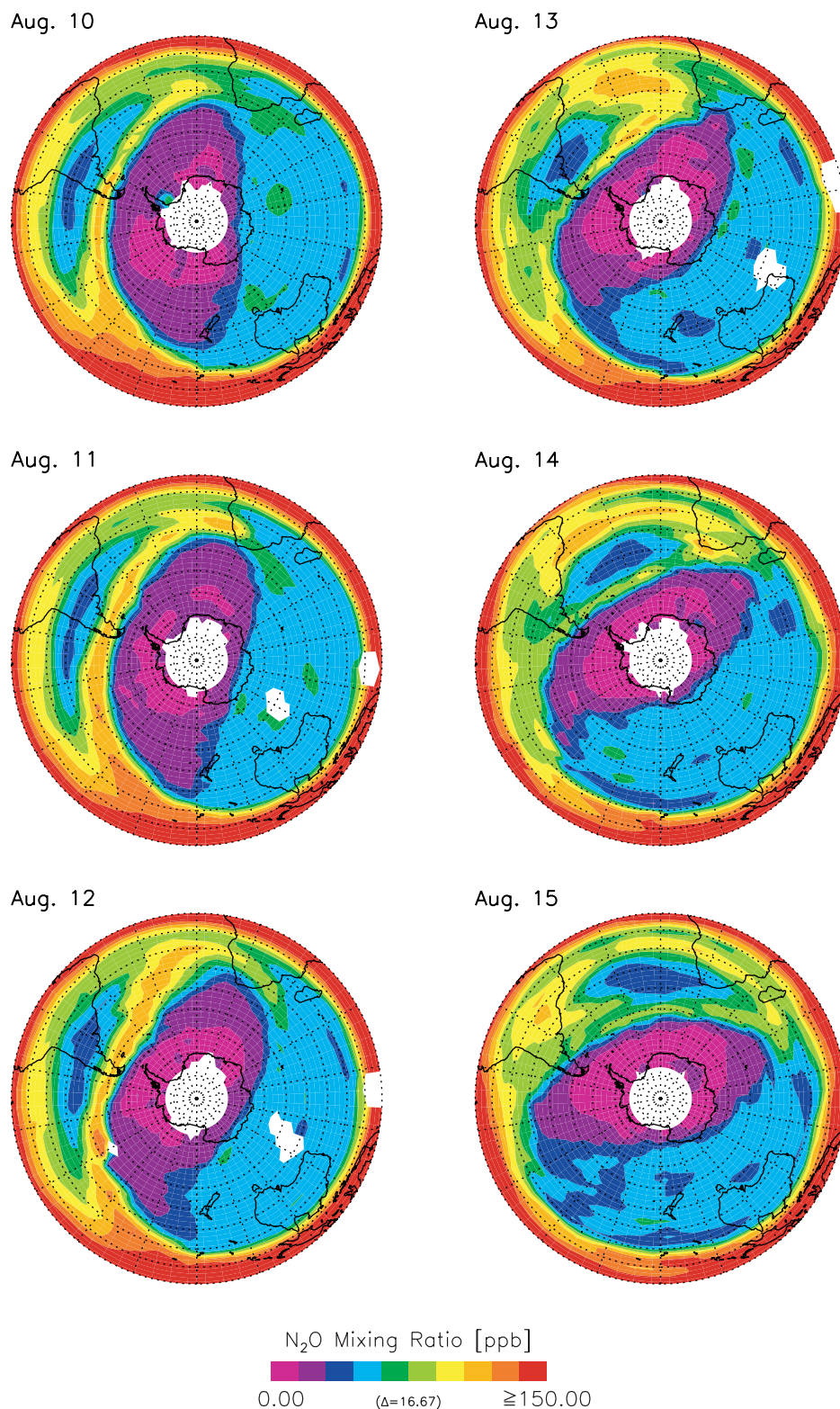
Figure 6. Time sequence of CRISTA-2 N_2O mixing ratio values at 10 hPa (10 August to 15 August) in the Southern Hemisphere. The observations shown in each plot were made over a time span of 24 hours (level-2 product). The distributions were obtained by interpolating the CRISTA-2 level-2 data onto a regular grid with a resolution of 2.5° in latitude and 5.6° in longitude. The interpolation was performed by applying a two-dimensional weighting function, which resembles a triangle function with a half width of 12° in longitude and 4° in latitude. Blank areas indicate grid points where no measured data are available inside the nonzero region of the weighting function.
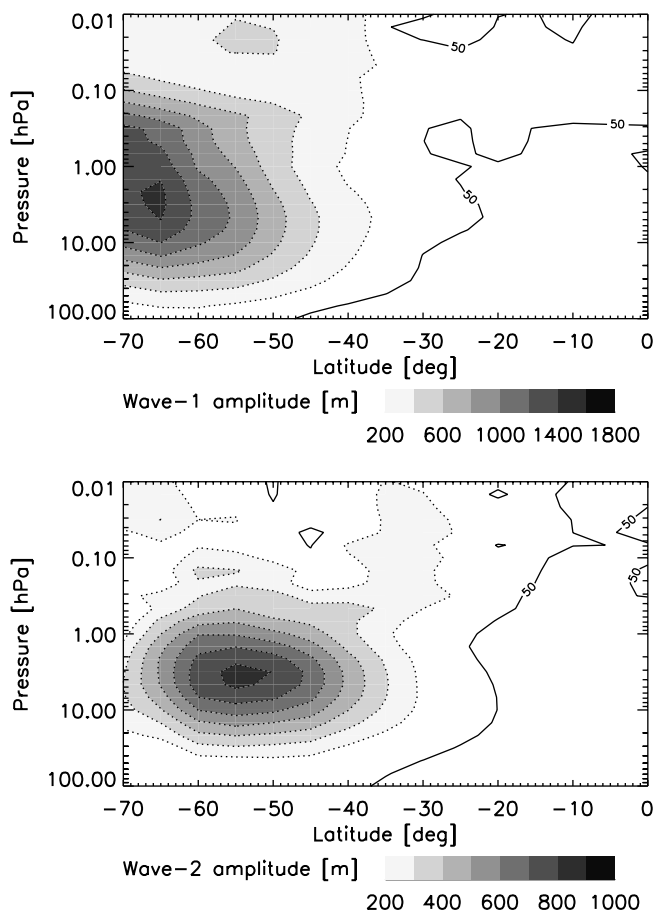
Figure 7. Wave-1 (upper panel) and wave-2 (lower panel) geopotential perturbation amplitudes. Mean amplitudes are shown for the CRISTA-2 mission (9 August through 15 August) by a gray scale map. In addition, contour lines showing small amplitudes (50 m) are included in order to provide more information on the height distribution in the tropics.

line), where the tropical transport barrier exhibits a large leak.

[14] As time proceeds and wave activity in the stratosphere becomes less pronounced (Figure 4), the interaction of the south polar vortex with the tropics becomes weakened. The remnants of tropical tongue drawn up by the earlier strong interaction (10, 11 August) start to circle around the polar vortex and are transported toward the tip of South Africa. A relatively small part of the tropical air mass is transported further poleward (see 12 August) around the vortex. However, most of the air is transported equatorward and then back westward by the tropical wind field, becoming trapped in an anticyclone composed of westerlies associated with the vortex edge in the south and tropical easterlies acting as a boundary in the north. The anticyclone propagates eastward with the traveling wave-1 and wave-2 structures. At the end of the CRISTA-2 observational period, enhanced filamentation can be seen inside the anticyclone, consistent with previous studies that showed filamentation of air drawn into an anticyclone [e.g., *Waugh*, 1993; *O'Neill et al.*, 1994; *Lahoz et al.*, 1996, and references therein]. The large- and medium-scale N_2O structures

observed by CRISTA are in good agreement with corresponding structures in potential vorticity fields derived from UK Met Office analyses [see *Günther et al.*, 2002, Figure 7].

4.2. Height Structure of Large-Scale Tracer Transport

[15] Latitude-height contour plots of wave-1 and wave-2 amplitudes as derived from the CRISTA geopotential perturbation field are shown in Figure 7. The amplitudes were calculated by means of a least-mean squares technique, which was also used in a previous analysis of *Ward et al.* [2000], who analyzed corresponding perturbation fields of temperature and ozone.

[16] To illustrate the relationship between the planetary wave amplitudes and the strength of the planetary-scale tongue of tropical air, Figure 8 shows trace gas distributions measured on 11 August in the altitude range from 1.0 hPa (50 km) to 46.4 hPa (22 km). Distributions of N_2O are shown for 2.15 hPa, 4.64 hPa, 10 hPa, and 21.5 hPa. Since N_2O is not yet retrieved above and below this altitude range, CH_4 and CFC-11 mixing ratios are shown for 1.0 hPa and 46.2 hPa, respectively. Comparison with Figure 7 shows that the strength of the tropical tongue is closely related to the combined wave-1 and wave-2 amplitudes. Wave-1 has a somewhat broader vertical structure than wave-2, but maximum amplitudes of both waves occur near the same pressure level (5 hPa). In particular, the unusually large wave-2 amplitudes at this time result in departures, much larger than usual, from a zonally symmetric flow at altitudes around 5 hPa. The strong decrease of the combined wave amplitudes above 2.15 hPa and below 10 hPa results in a significant reduction of transport from the tropics toward midlatitudes (as a result of a less pronounced equatorward displacement of the vortex edge). This is demonstrated in Figure 8 by the transition from 10 hPa to 21.5 hPa. The pronounced tongue of tropical air at 10 hPa becomes rather weak at 21.5 hPa due to decreasing wave amplitudes.

5. Quantitative Transport Studies Based on Assimilated N_2O Fields

[17] Quantitative transport studies require the interpolation of the asynoptic CRISTA data to common times and to a regular spatial grid (level 3 product). Due to the high data density and the global coverage, CRISTA trace gas fields are especially suited to mapping techniques based on trace gas assimilation. CRISTA synoptic maps of long-lived tracers have therefore been generated by means of a sequential trace gas assimilation method which has been developed for quantitative analyses of trace gas transport and photochemical processes [see *Riese et al.*, 1999b, 2000]. The assimilation system combines the chemistry and the transport codes of the National Center for Atmospheric Research (NCAR) Research on Ozone in the Stratosphere and its Evolution (ROSE) model [e.g., *Rose and Brasseur*, 1989; *Smith*, 1995] with analyzed wind and temperature fields provided by the UK Met Office. The sequential system uses a horizontal resolution of 2.5° in latitude and 5.6° in longitude, and a vertical resolution of about 2.7 km. Due to the high spatial resolution of CRISTA, trace gas mixing ratios are frequently updated by observed values at all model grid points inside the atmospheric region sampled by the instrument.
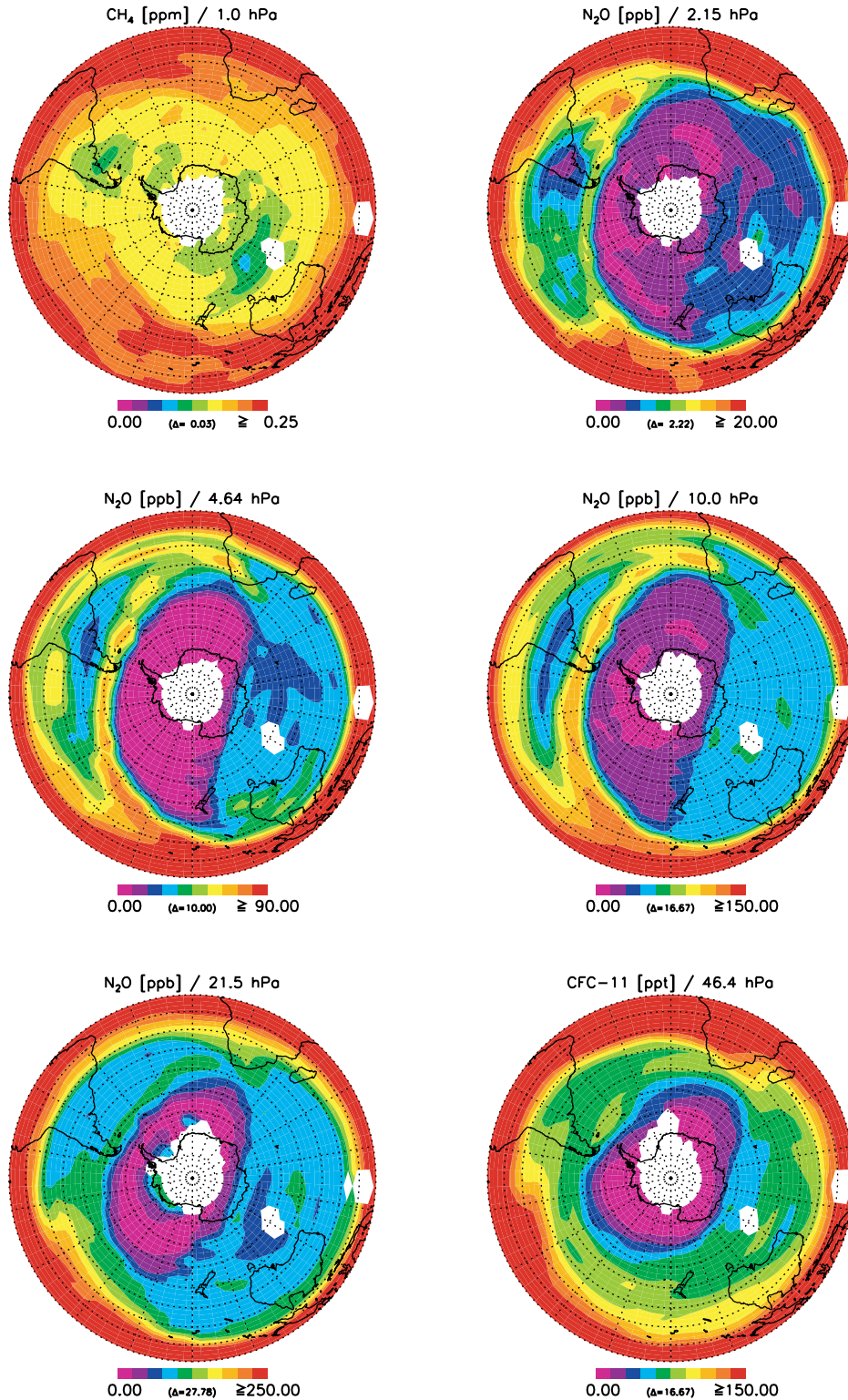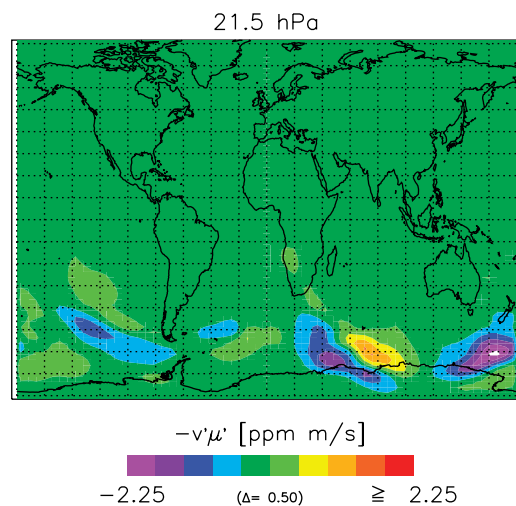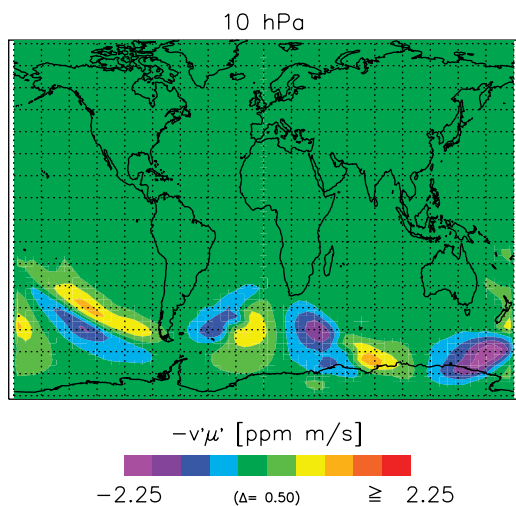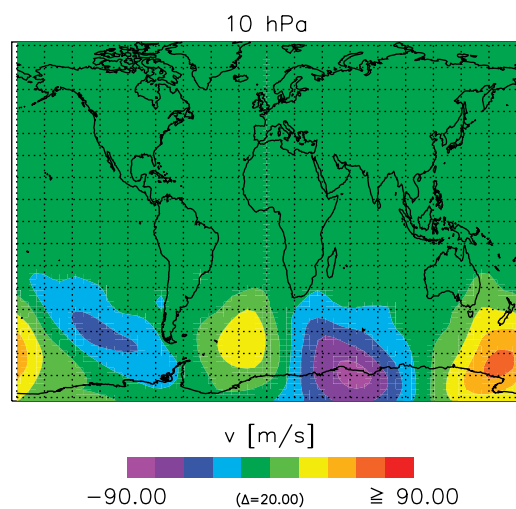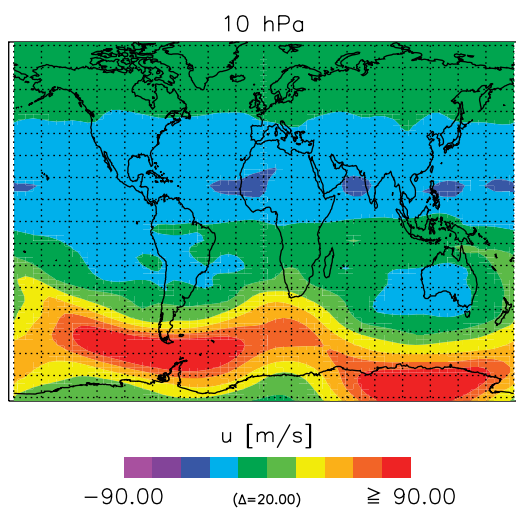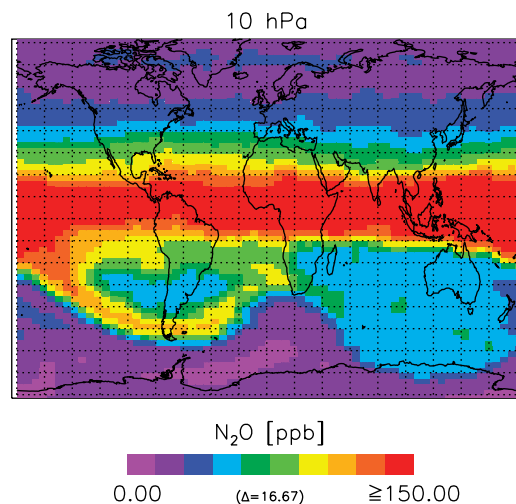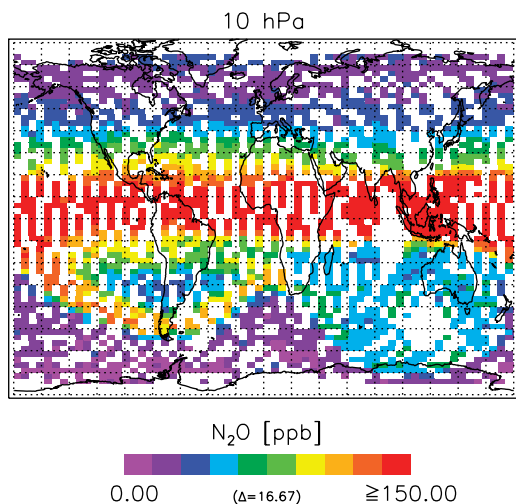
Figure 8. Altitude dependence of the planetary-scale tongue of tropical air observed by CRISTA-2. Shown are asynoptic trace gas distributions (level 2) for 11 August 1997: CH$_4$ at 1 hPa, N$_2$O at 2.15 hPa, 4.64 hPa, 10 hPa, and 21.5 hPa, and CFC-11 at 46.4 hPa. (For details about the mapping procedure see legend of Figure 6).

[18] The main advantage of the assimilation approach is the availability of wind, temperature, and trace gas data on the same spatial and temporal grid. This allows for calculations of transport quantities such as eddy fluxes of tracers [see *Riese et al.*, 1999b]. To illustrate the advantages of trace gas fields obtained from sequential assimilation, the upper row of Figure 9 shows a comparison of asynoptic N$_2$O observations at 10 hPa for 11 August (left side) with a

10 hPa

N$_2$O [ppb]

0.00   (Δ=16.67)   ≧150.00

10 hPa

N$_2$O [ppb]

0.00   (Δ=16.67)   ≧150.00

10 hPa

u [m/s]

−90.00   (Δ=20.00)   ≧ 90.00

10 hPa

v [m/s]

−90.00   (Δ=20.00)   ≧ 90.00

10 hPa

−v'μ' [ppm m/s]

−2.25   (Δ= 0.50)   ≧ 2.25

21.5 hPa

−v'μ' [ppm m/s]
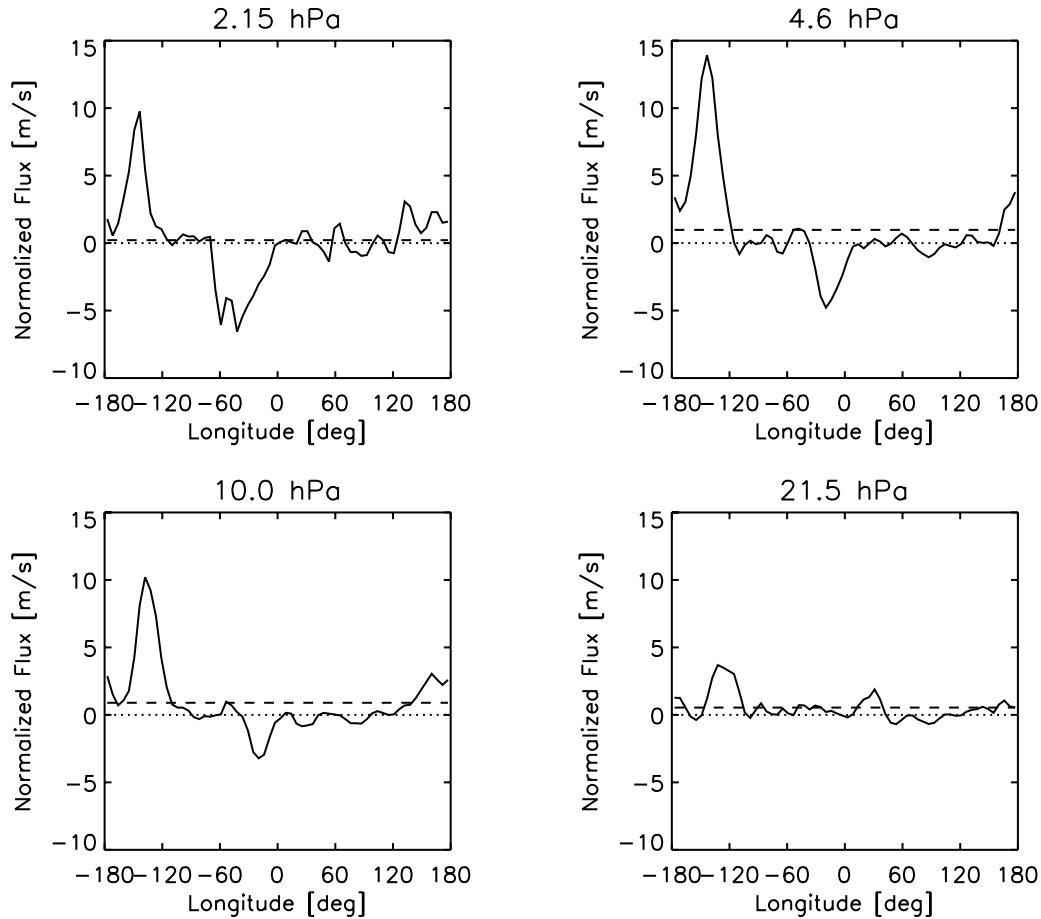
−2.25   (Δ= 0.50)   ≧ 2.25

Figure 10. Longitudinal plots of the N_2O flux term $-\overline{v'\mu'/\overline{\mu}}$ (solid lines) for 11 August 0000 UT at four pressure levels: 2.15 hPa 4.64 hPa , 10.0 hPa, and 21.5 hPa. All data represent averages for the latitudinal band from 40°S to 20°S. The zonally averaged flux ($-\overline{v'\mu'}/\overline{\mu}$) is also shown (dashed lines). For more details see text.

corresponding synoptic distribution for 11 August (0000 UT) obtained from the assimilation system. The asynoptic observations are projected onto the spatial grid of the chemical transport model (for details see figure caption). Trace gas values (colored rectangles) are only shown for those grid points which are the nearest neighbor of at least one observation. The size of single colored (or blank) rectangles in Figure 9 corresponds to the model resolution of 5.65° in longitude and 2.5° in latitude. While the figure suggests that the measurement net on 11 August is less dense than the model grid, this is not actually the case. The blank areas result mainly from the irregular distribution of

the measured values. The number of measured values is about the same as the number of model grid points. In the assimilated distribution (right side of upper row) mixing ratio values of N_2O are available at all grid points. The values represent the synoptic model forecast for 11 August (0000 UT) based on previous observations and measured information transported by the UKMO wind field. The associated zonal and meridional components of the wind field at 10 hPa are presented in the middle row of Figure 9. The horizontal wind fields reflect well the details of the large-scale tropical tongue shown in the upper row of Figure 9.

Figure 9. (opposite) (Upper panel) Comparison of asynoptic N_2O values observed by CRISTA-2 with corresponding assimilated N_2O values at 10 hPa. The observations were made over a time span of 24 hours (10 August, 0012 UT through 11 August, 0012 UT). The asynoptic CRISTA observations were interpolated onto the model grid, which has a resolution of 2.5° in latitude and 5.6° in longitude. For the interpolation a two-dimensional weighting function was applied, which resembles a triangle function with a half width of 2.8° in longitude and 1.25° in latitude. Through this approach, values are calculated only for those grid points, which are the nearest neighbor of at least one observation. Blank areas indicate grid points which are not nearest neighbor of an observed value. The assimilated data (on the right) represent a synoptic map (11 August, 0000 UT). (Middle panel) Horizontal wind fields at 10 hPa for 11 August, 0000 UT. Zonal winds are shown on the left and meridional winds on the right. (Lowest panel) Horizontal distribution of the N_2O eddy flux term ($-\overline{v'\mu'}$) at 10 hPa (left) and at 21.5 hPa (right) for 11 August 0000 UT. The maps shown in this plate cover longitudes from $-180°$ to $+180°$E and latitudes from $-80°$ to $+80°$. For more details see text.

[19] Transport analyses based on the Transformed Eulerian Mean (TEM) framework [e.g., *Andrews et al.*, 1987] indicate that eddy forcing in the tropics and at middle latitudes results almost entirely from the horizontal flux component M_y [e.g., *Randel et al.*, 1994]:

$$M_y = -\rho\left(\overline{v'\mu'} - \frac{R}{H}\frac{\overline{v'T'}}{N^2}\overline{\mu}_z\right) \quad (1)$$

[20] In equation (1), μ represents the trace gas mixing ratio, v is the meridional velocity, ρ stands for the atmospheric density, T for the atmospheric temperature, R is the gas constant, H is the scale height, N is the Brunt-Vaisala frequency, and z is the altitude. Overbars denote zonal means. Primes denote deviations from the zonal mean values.

[21] The pronounced tongue of tropical air results in positive N_2O flux in the subtropics. The flux term associated with N_2O mixing ratio structures $(-v'\mu')$ exhibits intense longitudinal variations as shown in the lowest panel of Figure 9 for the 10 hPa and the 21.5 hPa pressure levels. At middle and high latitudes, the flux pattern results in a cell structure with fluxes changing direction between two adjacent cells. The N_2O flux associated with the pronounced tropical tongue of air is considerably stronger at 10 hPa than at 21.5 hPa, as a result of the altitude dependence of the combined wave-1 and wave-2 amplitudes (see Figure 7).

[22] Longitudinal plots of the term $-\overline{v'\mu'}/\overline{\mu}$ averaged over the latitudinal band from $40°S$ to $20°S$ are shown in Figure 10 (solid lines) for four pressure levels (2.15 hPa, 4.6 hPa, 10 hPa, and 21.5 hPa). At each pressure level, the flux term $-v'\mu'$ has been divided by the zonal mean N_2O mixing ratio value $\overline{\mu}$ (averaged over the same latitudinal band) in order to obtain a comparison of relative magnitudes. The results indicate the large contribution of the tropical tongue area to the total flux. At 4.6 hPa and 10 hPa, about 70% of the total flux results from a longitudinal interval of about $40°$ centered around the longitude of the maximum flux contribution (at $130°W$). For comparison, the magnitude of the zonally averaged flux $-\overline{v'\mu'}/\overline{\mu}$ is shown in each plot by a dashed line. A good correspondence of the altitude dependence of $-\overline{v'\mu'}/\overline{\mu}$ with the altitude dependence of the combined wave-1 and wave-2 amplitudes (Figure 7) is found.

6. Summary

[23] CRISTA-2 observations were made in the Southern Hemisphere winter during a period when horizontal mixing ratio gradients in the area of the subtropical transport barrier were tightened and shifted toward low latitudes (down to $15°S$). Such a situation is usually characterized by relatively quiet mixing ratio fields, since interactions of the polar vortex with the subtropics are uncommon. However, due to extremely large amplitudes of both wave-1 and wave-2, and associated large displacement of the edge of the polar vortex toward the tropics, considerable trace gas flux occurred from the tropics into midlatitudes. The presence of both steep mixing ratio gradients in the tropics and large displacements of the strong polar vortex allowed for a detailed study of the interaction of the vortex edge with the tropics.

[24] Largest flux values occur in the altitude range from 2.15 to 10 hPa, where both wave-1 (about 1000 m at $55°S$)

and wave-2 (about 800 m at $55°S$) have largest amplitudes. The unusually large wave-2 amplitudes at this time result in much larger than usual departures from a zonally symmetric flow. The large wave-2 amplitude results in elongation of the polar vortex at two longitudinal locations $180°$ apart. The relative phase of wave-2 and wave-1 increases this displacement at one location (see Figure 6). Favorable phase alignment leads to the creation of a strong anticyclone drawing up the tropical air. CRISTA-2 observations highlight the importance of such transport events for trace gas eddy-transport in the Southern Hemisphere winter stratosphere.

References

Andrews, D. J., J. R. Holton, and C. B. Leovy, *Middle Atmosphere Dynamics, Int. Geophys. Ser.*, Academic, San Diego, Calif., 489 pp., 1987.

Grossmann, K. U., D. Offermann, O. Gusev, J. Oberheide, M. Riese, and R. Spang, The CRISTA-2 mission, *J. Geophys. Res.*, 107, this issue, 2002.

Günther, G., D. S. McKenna, and R. Spang, The meteorological conditions of the stratosphere for the CRISTA2 campaign (August 1997), *J. Geophys. Res.*, 107, this issue, 2002.

Haynes, P. H., C. J. Marks, M. E. McIntyre, T. G. Shepard, and T. G. Shine, On the "downward control" of extratropical diabatic circulations and eddy-induced mean zonal forces, *J. Atmos. Sci.*, 48, 651–678, 1991.

Lahoz, W. A., A. O'Neill, A. Heaps, V. D. Pope, R. Swinbank, R. S. Harwood, L. Froidevaux, W. G. Read, J. W. Water, and G. E. Peckham, Vortex dynamics and the evolution of water vapour in the stratosphere of the southern hemisphere, *Q. J. R. Meteorol. Soc.*, 122, 423–450, 1996.

Leovy, C. B., and P. J. Webster, Stratospheric long waves: Comparison of thermal structure in the Northern and Southern hemispheres, *J. Atmos. Sci.*, 33, 1624–1638, 1976.

Manney, G. L., J. D. Farrara, and C. R. Mechoso, The behavior of Wave 2 in the southern hemispheric stratosphere during late winter and early spring, *J. Atmos. Sci.*, 48, 976–998, 1991.

McIntyre, M. E., and T. N. Palmer, Breaking planetary waves in the stratosphere, *Nature*, 305, 593–600, 1983.

Oberheide, J., G. A. Lehmacher, D. Offermann, K. U. Grossmann, H. Manson, C. E. Meek, J. Schmidlin, W. Singer, P. Hoffman, and R. A. Vincent, Geostrophic wind fields in the stratosphere and mesosphere from satellite data, *J. Geophys. Res.*, 107, this issue, 2002.

Offermann, D., K. U. Grossmann, P. Barthol, P. Knieling, M. Riese, and R. Trant, The CRyogenic Infrared Spectrometers and Telescopes for the Atmosphere (CRISTA) experiment and middle atmosphere variability, *J. Geophys. Res.*, 104, 16,311–16,325, 1999.

O'Neill, A., W. L. Grose, V. D. Pope, H. Maclean, and R. Swinbank, Evolution of the stratosphere during Northern winter 1991–92 as diagnosed from U. K. Meteorological Office analyses, *J. Atmos. Sci.*, 51, 2800–2817, 1994.

Randel, W. J., J. C. Gille, A. E. Roche, J. B. Kumer, J. L. Mergenthaler, J. W. Waters, E. F. Fishbein, and W. A. Lahoz, Stratospheric transport from the tropics to middle latitudes by planetary wave mixing, *Nature*, 365, 533–535, 1993.

Randel, W. J., B. A. Boville, J. C. Gille, P. L. Bailey, S. T. Massie, J. B. Kumer, J. L. Mergenthaler, and A. E. Roche, Simulation of stratospheric N_2O in the NCAR CCM2: Comparison with CLAES data and global budget analysis, *J. Atmos. Sci.*, 51, 2834–2845, 1994.

Riese, M., R. Spang, P. Preusse, M. Ern, M. Jarisch, D. Offermann, and K. U. Grossmann, Cryogenic Infrared Spectrometers and Telescopes for the Atmosphere (CRISTA) data processing and atmospheric temperature and trace gas retrieval, *J. Geophys. Res.*, 104, 16,311–16,325, 1999a.

Riese, M., X. Tie, G. Brasseur, and D. Offermann, Three-dimensional simulations of stratospheric trace gas distributions measured by CRISTA, *J. Geophys. Res.*, *104*, 16,419–16,435, 1999b.

Riese, M., V. Küll, X. Tie, G. Brasseur, D. Offermann, G. Lehmacher, and A. Franzen, Modeling of nitrogen species measured by CRISTA, *Geophys. Res. Lett.*, *27*, 2221–2225, 2000.

Rose, K., and G. Brasseur, A three-dimensional model of chemically active trace species in the middle atmosphere during disturbed winter conditions, *J. Geophys. Res.*, *96*, 16,387–16,403, 1989.

Smith, A. K., Numerical simulations of global variations of temperature, ozone, and trace species in the stratosphere, *J. Geophys. Res.*, *100*, 1253–1269, 1995.

Swinbank, R., and A. O'Neill, A stratosphere-troposphere data assimilation system, *Mon. Weather Rev.*, *122*, 686–702, 1994.

Trepte, C. R., R. E. Veiga, and M. P. McCormick, The poleward dispersal of Mount Pinatubo volcanic aerosol, *J. Geophys. Res.*, *98*, 18,563–18,573, 1993.

Ward, W. E., J. Oberheide, M. Riese, P. Preusse, and D. Offermann, Planetary wave two signatures in CRISTA II ozone and temperature data, *Geophys. Monogr.*, *123*, 319–325, 2000.

Waugh, D. W., Subtropical stratospheric mixing linked to disturbances in the polar vortices, *Nature*, *365*, 535–537, 1993.

Waugh, D. W., Seasonal variations of isentropic transport out of the tropical stratosphere, *J. Geophys. Res.*, *101*, 4007–4023, 1996.

————————————

V. Küll, J. Oberheide, and R. Spang, Physics Department, University of Wuppertal, Gausse-Strasse 20, D-42097 Wuppertal, Germany. (riese@wpos2.physik.uni)

G. L. Manney, Jet Propulsion Laboratory, California Institute of Technology, Pasadena, CA, USA.

M. Riese, Research Center Jülich, ICG-I: Stratosphere, 52425 Jülich, Germany. (m.riese@fz-juelich.de)

X. Tie, National Center for Atmospheric Research, Boulder, CO, USA.